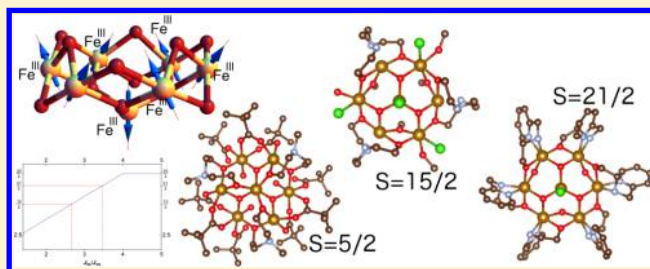


Magnetic Couplings in Spin Frustrated Fe^{III} Disklike ClustersJordan J. Phillips,[†] Juan E. Peralta,^{*,‡,†} and George Christou[§][†]Science of Advanced Materials, Central Michigan University, Mt. Pleasant, Michigan 48859, United States[‡]Department of Physics, Central Michigan University, Mt. Pleasant, Michigan 48859, United States[§]Department of Chemistry, University of Florida, Gainesville, Florida 32611-7200, United States

S Supporting Information

ABSTRACT: Using a methodology based on noncollinear coupled-perturbed density functional theory [J. Chem. Phys. 2013, 138, 174115] we calculate the magnetic exchange coupling parameters in a recently synthesized set of Fe^{III} disklike clusters [Inorg. Chem. 2011, 50, 3849–3851] to explain the unusually high ground-state spin found in the experiments. We show that the calculated exchange interactions for the new series of Fe^{III} disks present strikingly different trends compared to prior Fe^{III} disks. These differences are attributed to variations in the bridging ligands and the consequent structural changes in the complexes. The impact of these differences on the experimental ground-state spin of these complexes is rationalized using a simple classical spin model system and the calculated magnetic exchange couplings.



1. INTRODUCTION

Transition metal complexes featuring a large number of unpaired metal *d* electrons are of growing interest for applications such as spintronics¹ and magnetic memory storage.² One area of interest is the design of novel molecular magnets featuring high ground-state spins S_{tot} by tuning the different magnetic interactions through motivated structural perturbations. Disklike clusters such as Mn₇^{3,4} and Fe₇^{5–7} have attracted attention since they can feature a rich variety of spin ground-states depending on the particular competition between different *J* interactions and spin-frustration effects.⁸ Recently, a set of Fe^{III} disklike clusters with a six-pointed star topology were prepared by one of us (GC),⁹ given by [Fe₇O₃(OMe)₃-(hecn)₃Cl_{4.5}(MeOH)(H₂O)_{1.5}][FeCl₄]_{1/4} (shown in Scheme 1 as complex 2), and [Fe₇O₃(OH)₃Cl-(paeo)₆](Cl)(ClO₄)₄ (shown in Scheme 1 as complex 3), that feature an unusually large experimentally observed ground-state spin of $S_{\text{tot}} = 15/2$ and $21/2$, respectively. Except a recently reported $S_{\text{tot}} = 21/2$ disk prepared by Kizas et al.,¹⁰ typically Fe^{III} disks with antiferromagnetic interactions yield low-spin ground-states of $S_{\text{tot}} = 5/2$.^{5–7}

To gain insight into the origin of this unusually large spin, in this work we determine the magnetic interactions that take place in complexes 2 and 3 using Kohn–Sham density functional theory (KS-DFT)¹¹ calculations. For comparison, we also consider a prior studied Fe^{III} disklike cluster⁶ (Fe₇O₃(O₂CR₉(mda)₃(H₂O)₃; shown in Scheme 1 as complex 1 with ground-state spin of $S_{\text{tot}} = 5/2$. For clarity, the Heisenberg–Dirac^{12,13} spin Hamiltonian convention we will be employing is given by

$$\hat{H}_{\text{HD}} = - \sum_{i < j} J_{ij} \hat{\mathbf{S}}_i \cdot \hat{\mathbf{S}}_j \quad (1)$$

The reported magnetic couplings in this work were calculated using a recently developed methodology based on noncollinear coupled-perturbed KS-DFT.¹⁴ This methodology defines and computes the *J* couplings in terms of a Hessian of the KS energy with respect to local spin-rotation angles from the collinear high-spin (HS) reference configuration. For the purpose of making this work self-contained, we briefly remark on the relevant points of this method. To evaluate the derivative of the electronic energy with respect to local spin angles for a pair of metal atoms, we introduce the constraint condition

$$\frac{\mathbf{s}_1 \times \mathbf{s}_j}{s_1 s_j} = \theta_{1j} \hat{\mathbf{r}} \quad (2)$$

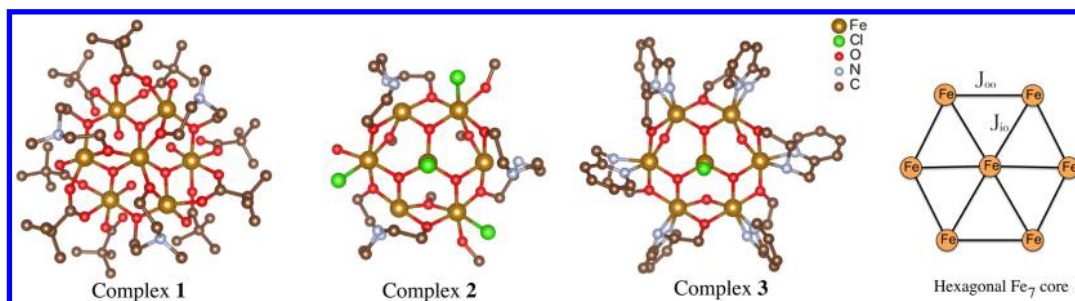
where \mathbf{s}_1 , \mathbf{s}_j are the local-spins¹⁵ of the 1st and *j*th metal atoms, and $1 < j \leq N$ (for the Fe₇ systems in this work, $N = 7$). Finding the stationary points of the Kohn–Sham energy subject to this constraint condition via Lagrange multipliers yields a modified single-particle eigenfunction problem which, assuming a collinear HS reference solution, simplifies to

$$(\hat{h} + \hat{J} + \hat{V}_{\text{XC}} - \sum_{1 < j} \lambda_{1j} \hat{f}_{1j}) \psi_k = \epsilon_k \psi_k \quad (3)$$

with

Received: August 19, 2013

Published: November 12, 2013

Scheme 1. Structures of Complexes 1–3 (with H Atoms Removed) and Simplified Hexagon Structure for the Fe₇ Core

$$\hat{f}_{1j} = -\frac{\hat{\sigma}_1^x}{s_1} + \frac{\hat{\sigma}_j^x}{s_j} \quad (4)$$

In 3 and 4, $\hat{h} + \hat{J} + \hat{V}_{\text{XC}}$ is the standard KS Hamiltonian, λ_{ij} are the Lagrange multipliers, and $\hat{\sigma}$ are Pauli operators. Considering λ_{ij} to be small and solving the first-order coupled-perturbed equations for each of the perturbations, we obtain for the Fe₇ case a 6×6 Hessian matrix $[\mathbb{E}_\lambda]_{ij} = d^2 E_{\text{KS}} / (d\lambda_i d\lambda_j)$, the inversion of which gives the constraint Hessian $[\mathbb{E}_\theta]_{ij} = d^2 E_{\text{KS}} / (d\theta_i d\theta_j)$. The magnetic couplings parameters may then be obtained by inspection of the matrix elements of the constraint Hessian via

$$J_{ij} = -\frac{1}{S_i S_j} \frac{d^2 E}{d\theta_i d\theta_j}, \quad 1 \neq i \neq j$$

$$J_{ij} = \frac{1}{S_i S_j} \sum_l \frac{d^2 E}{d\theta_l d\theta_l}, \quad 1 = i \neq j \quad (5)$$

For the complete details, we refer the reader to ref 14.

2. COMPUTATIONAL DETAILS

All calculations reported here were carried out using the Gaussian Development Version,¹⁶ using a hybrid of LDA (Slater exchange and Vosko, Wilk, Nusair correlation)¹⁷ given by $E_{\text{XC}} = aE_{\text{HF}}^{\text{X}} + (1 - a)E_{\text{LDA}}^{\text{X}} + E_{\text{LDA}}^{\text{C}}$, where $a = 0.3$. This choice originates in the poor convergence properties of the first-order KS equations with noncollinear GGA kernels.^{14,18,19} Here we note that for the purpose of evaluating magnetic exchange couplings, any family of functionals (LDA, GGA, M-GGA) can show reasonable accuracy when admixed with about 30% Hartree–Fock exchange.^{20–26} The basis-sets employed in this work are as follows: For transition metals we employ the 6-311G* basis set, while for the O atoms we employ the 6-31G* basis set and the 3-21G for all the remaining atoms. It should be pointed out that magnetic couplings in KS-DFT have a weak dependence on the choice of basis.²⁷ All calculations are performed employing pure d and f functions (Gaussian keyword “Sd 7f”), without symmetry constraints (“nosymm”), and the numerical integration is done with a pruned grid of 99 radial shells and 590 angular points per shell (“grid = ultrafine”). The convergence criteria employed are as follows: The zeroth-order calculations are converged to 10^{-10} Hartrees variation in the energy, 10^{-10} RMS variation in the density matrix, and 10^{-8} maximum allowed variation in the density matrix elements, while the first-order calculations are converged to 10^{-8} RMS variation in the first-order commutator matrix, with a maximum allowed variation in the analytic second derivatives of 1 Hartree/ λ^2 (typical second derivatives values

are of order 10^3 Hartrees/ λ^2 for the systems considered in this work). The unrelaxed gas-phase geometrical structures of the complexes were obtained from the crystallographic data provided in ref 9 and are available as Supporting Information.

3. RESULTS AND DISCUSSION

To rationalize the spin ground-state of these systems, let us first consider an hexagonal model for the Fe₇^{III} disklike core (shown at the rightmost side of Scheme 1) where by symmetry there are two unique nearest-neighbor couplings, given by J_{oo} (the “outer–outer” coupling) and J_{io} (the “inner–outer” coupling), and both are assumed to be antiferromagnetic ($J_{io} < 0$ and $J_{oo} < 0$). It is useful to consider two idealized extremes, where $|J_{io}/J_{oo}| \ll 1$, and alternatively where $|J_{oo}/J_{io}| \ll 1$. In the former case, the outer–outer interactions will dominate and a classical model will give alternating antiferromagnetic ordering for the outer Fe atoms, leaving only the central Fe atom’s spin uncanceled, yielding $S_{\text{tot}} = 5/2$. In the latter case the inner–outer interactions will dominate and the outer ring atoms will be spin-aligned, with the central Fe antialigned to the ring, yielding $S_{\text{tot}} = 25/2$. In intermediate cases the strength of J_{io} and J_{oo} can be comparable and there will be different degrees of spin-frustration. Although the formally correct way of dealing with this problem is by finding the eigenstates and eigenvalues of the quantum spin Hamiltonian, a simple inspection of the classical ground-state energy in terms of the local magnetic moment orientations can give some insight into the degree of frustration for different exchange coupling ratios J_{io}/J_{oo} . It should be pointed out that classical spin models have been successfully employed to describe the magnetic properties of large Fe₇^{III} frustrated spin systems.²⁸ To inspect the solutions of the classical spin system, we have minimized the energy as a function of the spin orientations of the corresponding hexagonal Fe₇^{III} (Figure 1) classical model for different J_{io}/J_{oo} ratios using a simple Monte Carlo technique. In this model, while all solutions present coplanar spin vectors, the spin-frustrated solutions are characterized by noncollinear spin vectors as shown schematically in Figure 2. In Figure 1 we show the total spin S_{tot} of the lowest-energy solutions as a function of J_{io}/J_{oo} . We find that, within this model, frustrated high-spin solutions occur for $|J_{io}| \lesssim 4|J_{oo}|$ while for $|J_{io}| \gtrsim 4|J_{oo}|$ the spin of the system saturates at the highest value $S_{\text{tot}} = 25/2$, as expected. High-spin solutions that give $S_{\text{tot}} = 15/2$ (complex 2) and $S_{\text{tot}} = 21/2$ (complex 3) are expected for ratios $J_{io}/J_{oo} \sim 2.7$ and $J_{io}/J_{oo} \sim 3.5$, respectively.

Now let us consider our DFT results. Beginning with complex 1, in Figure 3 we show calculated magnetic couplings (cm^{-1}) for nearest-neighbors metal atoms. For this complex, three strong antiferromagnetic interactions can be identified between outer–outer Fe atoms (Fe2–Fe5, Fe3–Fe6, and Fe4–

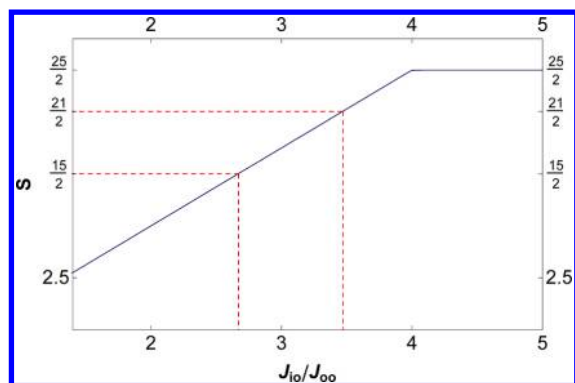


Figure 1. Ground-state total spin S_{tot} vs $J_{\text{io}}/J_{\text{oo}}$ for the classical Heisenberg model. The dashed lines indicate the location of $J_{\text{io}}/J_{\text{oo}}$ for complexes 2 and (experimental values of $S = 15/2$ and $21/2$, respectively) according to this model.

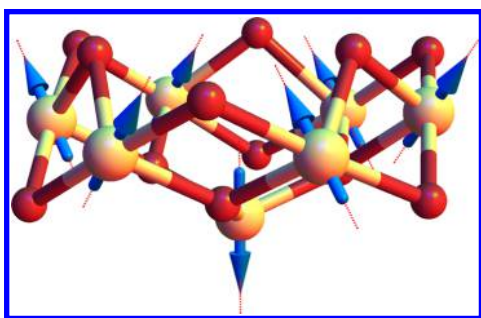


Figure 2. Lowest-energy classical spin configuration for complex 2 with $J_{\text{io}}/J_{\text{oo}} = 3$ (see text). Only the core structure is shown with Fe atoms in yellow and O in red.

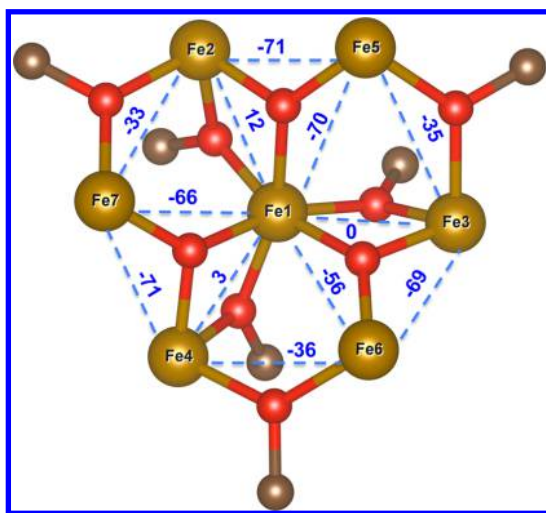


Figure 3. Calculated magnetic couplings (cm^{-1}) for complex 1.

Fe7), while another three strong antiferro-interactions are found between inner–outer Fe atoms (Fe1–Fe5, Fe1–Fe6, and Fe1–Fe7). The remaining three outer–outer interactions between peripheral Fe atoms are intermediate in magnitude, while the last three inner–outer interactions are weak or negligible. The exchange couplings in complex 1 favor a lowest-energy solution with alternating antiferromagnetic ordering for the outer Fe atoms as described in the previous paragraph, consistent with the experimentally observed $S_{\text{tot}} = 5/2$.

In Figure 4 we show the calculated magnetic couplings (cm^{-1}) for complexes 2 and 3. In this case, we can broadly identify two sets of antiferromagnetic interactions: Strong couplings between the central and outer Fe atoms bridged by $\mu_3\text{-O}^{2-}$, and weak couplings between the outer nearest-neighbor Fe atoms. The exchange interactions for complexes 2 and 3 are similar to each other but significantly different from those of 1: In the latter system, it is the outer–outer couplings that dominates with weak inner–outer couplings, while for 2 and 3 these trends are reversed and inner–outer interactions dominate.

From the classical model system discussed before and the calculated J couplings, we can straightforwardly infer that complex 2 and 3 tend toward the extreme case of $|J_{\text{oo}}| \ll |J_{\text{io}}|$, with a corresponding $S_{\text{tot}} = 25/2$, while complex 1 is qualitatively similar to the case $|J_{\text{io}}| \ll |J_{\text{oo}}|$ with a corresponding $S_{\text{tot}} = 5/2$. Therefore, the larger value of J_{io} in complexes 2 and 3 than in complex 1 confirms a higher spin ground-state in 2 and 3 than in 1, in agreement with the experimentally observed trends. A closer analysis of the calculated J_{io} and J_{oo} couplings yields an average J_{io} to average J_{oo} ratio for complex 2 of 8.5, while the same ratio for complex 3 is 9.9. According to Figure 1, these $J_{\text{io}}/J_{\text{oo}}$ ratios correspond in both cases to a saturated value of $S_{\text{tot}} = 25/2$. This indicates that even though our calculated J couplings can explain the high-spin observed experimentally for complexes 2 and 3, according to the classical model (Figure 1) the strong antiferromagnetic interactions might be overestimated with respect to the weak interactions. However, our DFT calculations successfully predict a higher $J_{\text{io}}/J_{\text{oo}}$ ratio for complex 3 than for complex 2, consistent with the higher S_{tot} in 3 than in 2. Therefore, besides all the approximations involved, our calculated couplings correctly predict the ordering of the ground-state spin of the three complexes.

Why are the exchange coupling interactions in 2 and 3 so different from those in 1? Couplings in oxo-bridged dinuclear Fe_2^{III} complexes are known to be dependent on both the Fe–O bond lengths and, to a lesser but still significant extent, on the Fe–O–Fe angles, and various empirical and semiempirical magnetostructural relationships have been formulated to estimate J values from these parameters.^{29,30} The main difference between compounds 1 and 2/3 is the coordination of the central Fe atom, which is six-coordinate with distorted octahedral geometry in 1 and four-coordinate with distorted tetrahedral geometry in 2 and 3. Since metal–ligand bond distances decrease with decreasing coordination number, if other factors are equal, it is expected that the Fe–O bond lengths to the central Fe atom will be significantly shorter in 2 and 3 than in 1. This is indeed the case, with the XRD Fe–O bond ranges being 1.987(4)–2.023(4) Å (average 2.005 Å), 1.844(4)–1.856(4) Å (average 1.849 Å), and 1.866(3)–1.885(3) Å (average 1.875 Å) for 1–3, respectively. Decreased Fe–O bond lengths to the central Fe atom in 2 and 3 will serve to increase the other Fe–O lengths in the Fe_7 core, and the net effect is expected to be an increase in J_{io} and a decrease in J_{oo} relative to 1. The changes in the peripheral ligands bridging the outer Fe atoms will also have an effect, primarily on J_{oo} . For example, it is known from studies on a family of Mn_7 clusters, which are structurally similar to the present Fe_7 clusters, that changing the identity of the peripheral ligands can have small but significant impact on the J values in the magnetic core of the molecule, altering the ground-state spin from $S_{\text{tot}} = 11$ to 16.^{29,30} It is also worth pointing out that there is appreciably good qualitative agreement between the calculated DFT

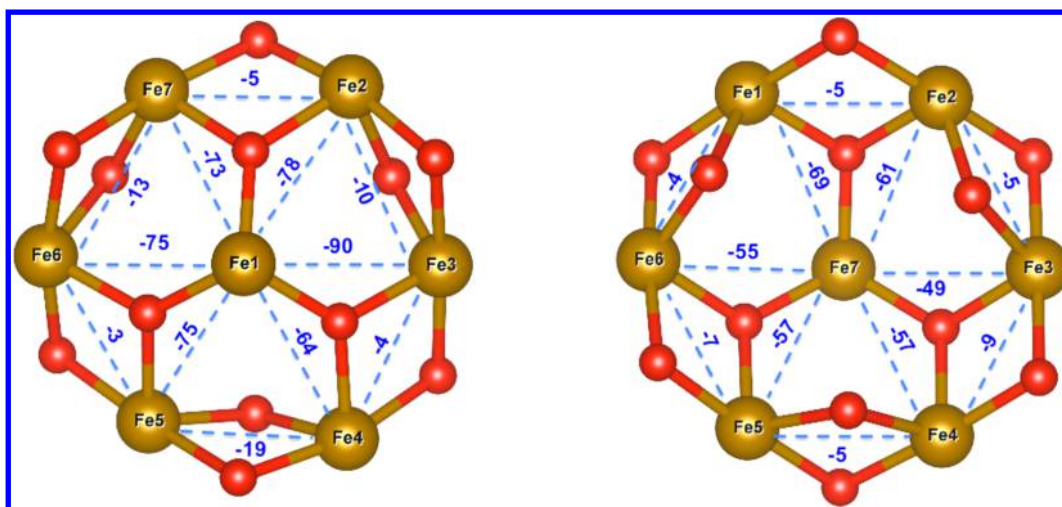


Figure 4. Calculated magnetic couplings (cm^{-1}) for complexes 2 (left) and 3 (right).

couplings reported herein and those determined for 1–3 from application of the magnetostructural relationship of Weihe and Güdel³⁰ as reported by Mukherjee et al.⁹

4. CONCLUSIONS

A novel methodology, based on linear-response density functional theory, has been employed to explain the higher ground-state spin found in two Fe_7^{III} disklike complexes (2 and 3) by evaluating their magnetic exchange coupling parameters. Our calculations reveal that the magnetic exchange interactions of the new complexes 2 and 3 are qualitatively different compared to those of the low-spin complex 1, which leads to their significantly higher ground-state spins, in agreement with experimental observations. Our analysis shows that the origin of the different trends in the couplings is due to the structural modification of the bridging ligands in the central and periphery of the disks, which results in the suppression of the strength of the antiferromagnetic interactions between the outer Fe atoms and an enhancement of the interactions between the central and outer Fe atoms.

■ ASSOCIATED CONTENT

Supporting Information

Geometrical structures of complexes 1, 2, and 3 used in the calculations is provided. This material is available free of charge via the Internet at <http://pubs.acs.org/>.

■ AUTHOR INFORMATION

Corresponding Author

*E-mail: juan.peralta@cmich.edu.

Notes

The authors declare no competing financial interest.

■ ACKNOWLEDGMENTS

Work at CMU was supported by NSF DMR-1206920. Work at UF was supported by NSF DMR-1213030.

■ REFERENCES

- (1) Heersche, H. B.; de Groot, Z.; Folk, J. A.; van der Zant, H. S. J.; Romeike, C.; Wegewijs, M. R.; Zobbi, L.; Barreca, D.; Tondello, E.; Cornia, A. *Phys. Rev. Lett.* **2006**, *96*, 206801.
- (2) Christou, G.; Gatteschi, D.; Hendrickson, D.; Sessoli, R. *MRS Bull.* **2000**, *25*, 66–71.

- (3) Stamatatos, T. C.; Poole, K. M.; Foguet-Albiol, D.; Abboud, K. A.; O'Brien, T. A.; Christou, G. *Inorg. Chem.* **2008**, *47*, 6593–6595.
- (4) Stamatatos, T. C.; Foguet-Albiol, D.; Poole, K. M.; Wernsdorfer, W.; Abboud, K. A.; O'Brien, T. A.; Christou, G. *Inorg. Chem.* **2009**, *48*, 9831–9845.
- (5) Jones, L. F.; Jensen, P.; Moubaraki, B.; Berry, K. J.; Boas, J. F.; Pilbrow, J. R.; Murray, K. S. *J. Mater. Chem.* **2006**, *16*, 2690–2697.
- (6) Datta, S.; Betancur-Rodriguez, A.; Lee, S.-C.; Hill, S.; Foguet-Albiol, D.; Bagai, R.; Christou, G. *Polyhedron* **2007**, *26*, 2243–2246.
- (7) Ako, A. M.; Waldmann, O.; Mereacre, V.; Klöwer, F.; Hewitt, I. J.; Anson, C. E.; Güdel, H. U.; Powell, A. K. *Inorg. Chem.* **2007**, *46*, 756–766.
- (8) Kahn, O. *Chem. Phys. Lett.* **1997**, *265*, 109–114.
- (9) Mukherjee, S.; Bagai, R.; Abboud, K. A.; Christou, G. *Inorg. Chem.* **2011**, *50*, 3849–3851.
- (10) Kizas, C. M.; Papatriantafyllopoulou, C.; Pissas, M.; Sanakis, Y.; Javed, A.; Tasiopoulos, A. J.; Lampropoulos, C. *Polyhedron* **2013**, *64*, 280–288.
- (11) (a) Hohenberg, P.; Kohn, W. *Phys. Rev.* **1964**, *136*, B864–B871. (b) Kohn, W.; Sham, L. J. *Phys. Rev.* **1965**, *140*, A1133–A1138.
- (12) Heisenberg, W. *Z. Phys. A Hadrons Nuclei* **1928**, *49*, 619–636.
- (13) Dirac, P. A. M. *Proc. R. Soc. London, Ser. A* **1929**, *123*, 714–733.
- (14) Phillips, J. J.; Peralta, J. E. *J. Chem. Phys.* **2013**, *138*, 174115.
- (15) (a) Clark, A. E.; Davidson, E. R. *J. Chem. Phys.* **2001**, *115*, 7382. (b) Davidson, E. R.; Clark, A. E. *Mol. Phys.* **2002**, *100*, 373–383.
- (16) Frisch, M. J.; Trucks, G. W.; Schlegel, H. B.; Scuseria, G. E.; Robb, M. A.; Cheeseman, J. R.; Scalmani, G.; Barone, V.; Mennucci, B.; Petersson, G. A.; Nakatsuji, H.; Caricato, M.; Li, X.; Hratchian, H. P.; Izmaylov, A. F.; Bloino, J.; Zheng, G.; Sonnenberg, J. L.; Liang, W.; Hada, M.; Ehara, M.; Toyota, K.; Fukuda, R.; Hasegawa, J.; Ishida, M.; Nakajima, T.; Honda, Y.; Kitao, O.; Nakai, H.; Vreven, T.; Montgomery, J. A., Jr.; Peralta, J. E.; Ogliaro, F.; Bearpark, M.; Heyd, J. J.; Brothers, E.; Kudin, K. N.; Staroverov, V. N.; Keith, T.; Kobayashi, R.; Normand, J.; Raghavachari, K.; Rendell, A.; Burant, J. C.; Iyengar, S. S.; Tomasi, J.; Cossi, M.; Rega, N.; Millam, J. M.; Klene, M.; Knox, J. E.; Cross, J. B.; Bakken, V.; Adamo, C.; Jaramillo, J.; Gomperts, R.; Stratmann, R. E.; Yazyev, O.; Austin, A. J.; Cammi, R.; Pomelli, C.; Ochterski, J. W.; Martin, R. L.; Morokuma, K.; Zakrzewski, V. G.; Voth, G. A.; Salvador, P.; Dannenberg, J. J.; Dapprich, S.; Parandekar, P. V.; Mayhall, N. J.; Daniels, A. D.; Farkas, O.; Foresman, J. B.; Ortiz, J. V.; Cioslowski, J.; Fox, D. J. *Gaussian Development Version, Revision H.13*; Gaussian, Inc., Wallingford, CT, 2010.
- (17) (a) Slater, J. *The Self-consistent Field for Molecules and Solids. Quantum Theory of Molecules and Solids*; McGraw-Hill: New York, 1974; Vol. 4. (b) Vosko, S. H.; Wilk, L.; Nusair, M. *Can. J. Phys.* **1980**, *58*, 1200–1211.

- (18) Shao, Y.; Head-Gordon, M.; Krylov, A. I. *J. Chem. Phys.* **2003**, *118*, 4807–4818.
- (19) Bernard, Y. A.; Shao, Y.; Krylov, A. I. *J. Chem. Phys.* **2012**, *136*, 204103.
- (20) Cabrero, J.; Calzado, C. J.; Maynau, D.; Caballol, R.; Malrieu, J. P. *J. Phys. Chem. A* **2002**, *106*, 8146–8155.
- (21) Calzado, C. J.; Cabrero, J.; Malrieu, J. P.; Caballol, R. *J. Chem. Phys.* **2002**, *116*, 3985–4000.
- (22) de, P. R.; Moreira, I.; Illas, F.; Martin, R. L. *Phys. Rev. B* **2002**, *65*, 155102.
- (23) Feng, X.; Harrison, N. M. *Phys. Rev. B* **2004**, *70*, 092402.
- (24) Phillips, J. J.; Peralta, J. E. *J. Chem. Phys.* **2011**, *134*, 034108.
- (25) Valero, R.; Illas, F.; Truhlar, D. G. *J. Chem. Theory Comput.* **2011**, *7*, 3523–3531.
- (26) Phillips, J. J.; Peralta, J. E. *J. Chem. Theory Comput.* **2012**, *8*, 3147–3158.
- (27) Yamanaka, S.; Kanda, K.; Saito, T.; Kitagawa, Y.; Kawakami, T.; Ehara, M.; Okumura, M.; Nakamura, H.; Yamaguchi, K. *Chem. Phys. Lett.* **2012**, *519–520*, 134–140.
- (28) Axenovich, M.; Luban, M. *Phys. Rev. B* **2001**, *63*, 100407.
- (29) Gorun, S. M.; Lippard, S. J. *Inorg. Chem.* **1991**, *30*, 1625–1630.
- (30) Weihe, H.; Güdel, H. U. *J. Am. Chem. Soc.* **1997**, *119*, 6539–6543.